*minerals*

MDPI

*Article*

# Nephrite from Xinjiang Qiemo Margou Deposit: Gemological and Geochemical Insights

**Ting Fang [1,2], Yuan Chang [1,2] and Mingxing Yang [1,2,*]**

1 Gemmological Institute, China University of Geosciences, Wuhan 430074, China; funtyfang@163.com (T.F.); gicchang@163.com (Y.C.)
2 Hubei Province Gem and Jewelry Engineering Technology Research Center, Wuhan 430074, China
* Correspondence: yangc@cug.edu.cn

**Abstract:** The nephrite belt in the Altun Mountain–Western Kunlun Mountain region, which extends about 1300 km in Xinjiang, NW China, is the largest nephrite deposit in the world. The Qiemo region in the Altun Mountains is a crucial nephrite-producing area in China, with demonstrated substantial prospects for future exploration. While existing research has extensively investigated secondary nephrite deposits in the Karakash River and native black nephrite deposits in Guangxi Dahua, a comprehensive investigation of black nephrite from original deposits in Xinjiang is lacking. Margou black-toned nephrite was recently found in primary deposits in Qiemo County, Xinjiang; this makes in-depth research on the characteristics of this mine necessary. A number of technical analytical methods such as polarizing microscopy, Ultra-Deep Three-Dimensional Microscope, electron microprobe, back-scattered electron image analysis, X-ray fluorescence, and inductively coupled plasma mass spectrometry were employed for this research. An experimental test was conducted to elucidate the chemical and mineralogical composition, further clarifying the genetic types of the black and black cyan nephrite from the Margou deposit in Qiemo, Xinjiang. The results reveal that the nephrite is mainly composed of tremolite–actinolite, characterized by Mg/(Mg + $Fe^{2+}$) ratios ranging from 0.86 to 1.0. Minor minerals include diopside, epidote, pargasite, apatite, zircon, pyrite, and magnetite. Bulk-rock rare earth element (REE) patterns exhibit distinctive features, such as negative Eu anomalies (δEu = 0.00–0.17), decreasing light REEs, a relatively flat distribution of heavy REEs, and low total REE concentrations (1.6–38.9 μg/g); furthermore, the Cr (6–21 μg/g) and Ni (2.5–4.5 μg/g) contents are remarkably low. The magmatic influence of granite appears to be a fundamental factor in the genesis of the magnesian skarn hosting Margou nephrite. The distinctive black and black cyan colors are attributed to heightened iron content, mainly associated with FeO (0.08~6.29 wt.%). Analyses of the chemical composition allow Margou nephrite to be classified as typical of magnesian skarn deposits.

**Keywords:** nephrite; tremolite–actinolite; chemical composition

check for updates

**Citation:** Fang, T.; Chang, Y.; Yang, M. Nephrite from Xinjiang Qiemo Margou Deposit: Gemological and Geochemical Insights. *Minerals* **2024**, *14*, 458. https://doi.org/10.3390/min14050458

Academic Editor: Evgeny Galuskin

Received: 8 February 2024
Revised: 22 April 2024
Accepted: 23 April 2024
Published: 26 April 2024



## 1. Introduction

The primary constituents of nephrite are the minerals of the amphibole group, belonging to the tremolite–actinolite–ferro-actinolite series, characterized by the general chemical formula of $Ca_2(Mg, Fe)_5Si_8O_{22}(OH)_2$. Nephrite has a characteristic tangled fibrous texture [1]. The predominant mineral in nephrite is tremolite, accompanied by minor minerals such as actinolite, diopside, talc, serpentine, epidote, clinozoisite, forsterite, coarse-grained tremolite, dolomite, quartz, magnetite, and pyrite [2–5]. Globally, nephrite deposits are found in various countries, including China, Canada, Russia, South Korea, Australia, New Zealand, Pakistan, and Poland [6–9]. In particular, in China, the most important nephrite deposits are located in Yutian County, Qiemo County, Ruoqiang County, Yulong Kashgar River, Karakashi River in the Hetian Region of Xinjiang, Golmud in Qinghai Province, Xiuyan in Liaoning Province, Panshi in Jilin Province, Tieli in Heilongjiang Province, Liyang in Jiangsu Province, Shimian County in Sichuan Province, Luanchuan in Henan Province, and Hualien in Taiwan Province [6–8]. Among them, the magnesium marble-type tremolite nephrite belt in western Kunlun of Xinjiang stands out as the world's largest and most economically valuable nephrite deposit [1,6,10–13].

Based on their genesis, nephrites can be classified into two distinct types: dolomite marble type (D-type) and serpentinite type (S-type) [1,10,14–16]. Serpentinite-type nephrite forms at the contact between serpentinized peridotite and acidic to intermediate intrusions or metasediments. Meanwhile, S-type nephrite, which is more widely distributed globally, has renowned and representative deposits in Hualian, Taiwan, Manasi, Xinjiang, China; East Sayan, Siberia, Russia; British Columbia, Canada; New Zealand; Poland; and Bulgaria. Meanwhile, dolomite marble-type nephrite is mainly found in the contact zones between magnesian marble and magmatic rocks [13–17]. The origin of nephrite deposits in the Xinjiang region is attributed to the contact metamorphism of magnesium carbonate rocks adjacent to local granite bodies [13,14]. The granodiorite and granite intrusions along the Western Kunlun Mountains of the Hetian Nephrite Belt, which extends for approximately 1300 km, played a critical role in the formation of nephrite [16]. Understanding the formation mechanism of nephrite provides valuable insights into elemental migration during skarn rock formation [18].

In the region of Xinjiang, the nephrite mineralization belt encompasses over 30 primary nephrite deposits, often associated with skarn and extensive hydrothermal alteration [18,19]. To date, systematic research on the mineral composition of black nephrite in primary skarn-type nephrite deposits has been limited [20]. Despite the abundance of black nephrite placer deposits in the Karakash River, there is a scarcity of reports on their occurrence in primary nephrite deposits [18]. This study focuses on Margou black and black cyan nephrite samples from the primary deposits in Qiemo County, Xinjiang, which offer valuable information due to their distinctive coloration and geological context. To enhance the research content, various analytical methods—including polarizing microscope analysis, electron microprobe analysis (EMPA), back-scattered electron image (BSE) analysis, X-ray fluorescence spectroscopy (XRF), and inductively coupled plasma mass spectrometry (ICP-MS)—are employed. This multi-faceted approach aims to elucidate the petrographic characteristics, chemical composition, and mineral constituents of Margou nephrite samples, contributing to a comprehensive understanding of their genesis.

## 2. Geological Setting

### *2.1. Margou Nephrite Deposit*

The study area is located in the northern part of the westernmost central line of the Altun Mountains in the Tarim Basin. It is located in the upper reaches of the Dasha River, about 150 kilometers east of Qiemo County, Xinjiang, and belongs to the Qiemo–Ruoqiang and Tianyu metallogenic belts (Figure 1). The ore belt is composed of multiple nephrite ore bodies with similar geological background and genesis, and it is often produced in the contact zone between Pre-Cambrian dolomitic marble and intermediate-acid granite intruded during the Hercynian orogeny [20].

The Margou nephrite mine, a recently discovered black cyan nephrite deposit situated in Qiemo County, Xinjiang Province, presents a distinct geological profile (Figure 2). The strata in the mining area encompass hornblende biotite gneiss and medium-thickness coarse-grained white marble (Figure 3A). Magmatic rocks in the region include light gray medium-grained monzonitic granite and diorite (Figure 3B). Stratigraphically, the direction of the strata is north–northwest, the tendency is northeast, and the dip angle is 70–80 degrees. Notably, the diorite exhibits veining at the contact between marble and gneiss. Black cyan nephrite mineralization occurs predominantly along the contact zone or bedding in the outer contact zone of monzonitic granite and dolomite marble. The associated alterations related to mineralization processes include potassic feldspathization, epidotization, tremolitization, serpentinization, and phlogopitization.

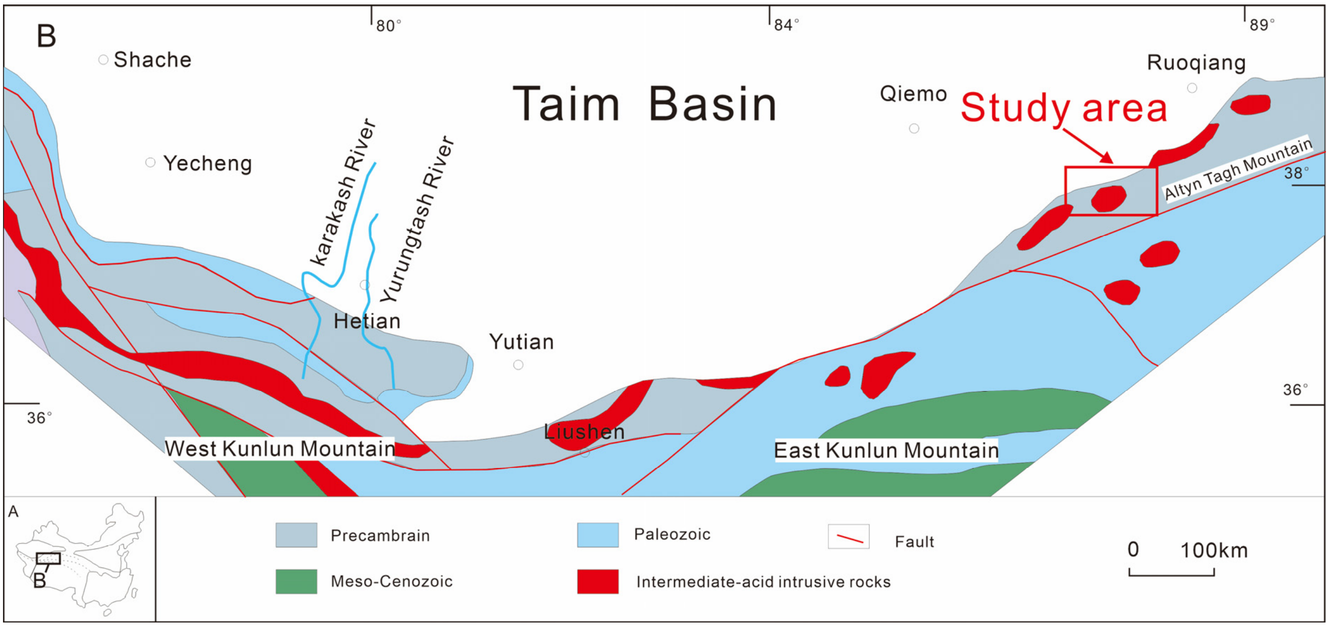


**Figure 1.** (**A**) Location of nephrite belt in the map of China. (**B**) Simplified geologic map of the Hetian Nephrite Belt, showing the scope of the research area (modified from [15,18,20]).

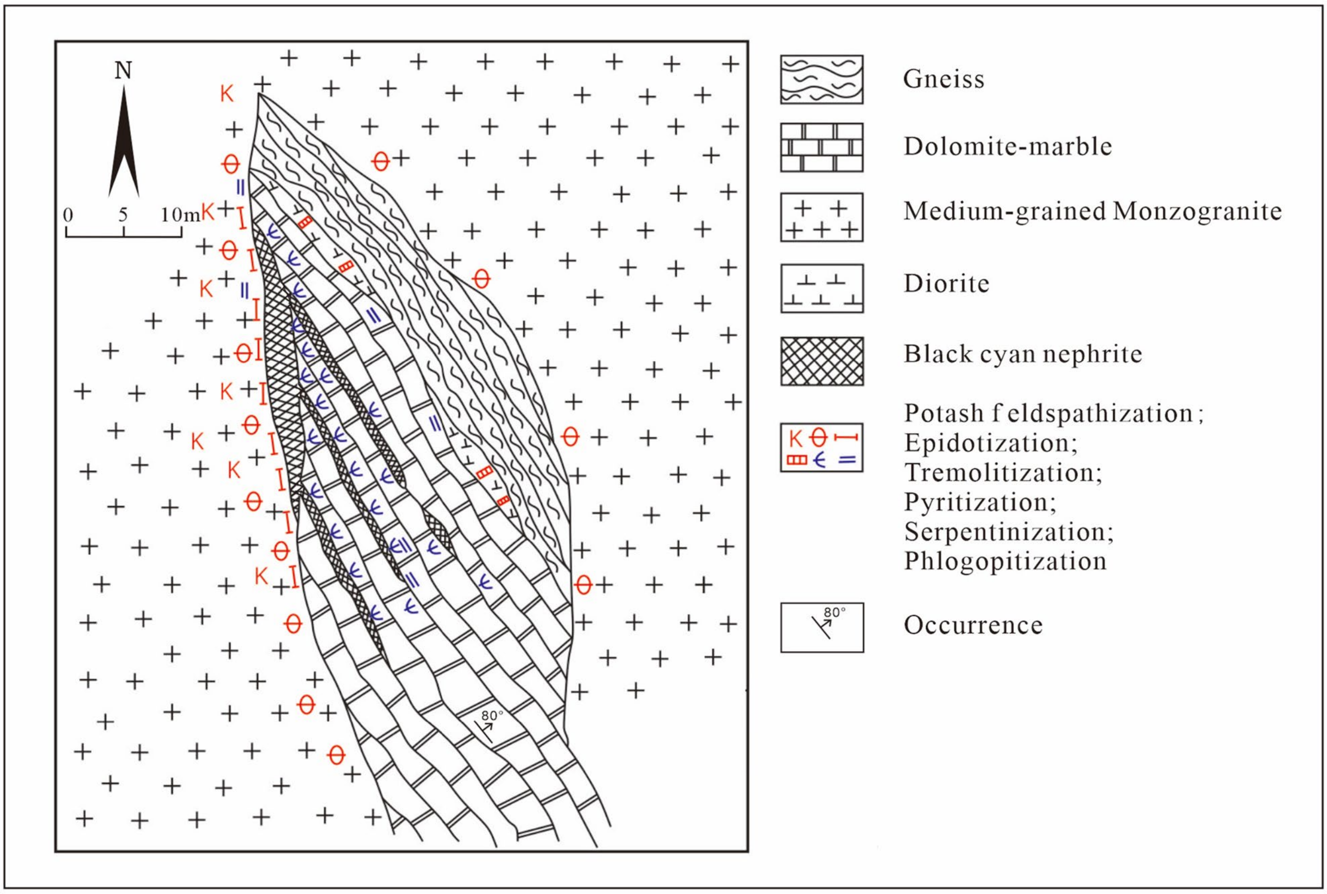


**Figure 2.** Plane geological sketch of the black cyan nephrite in Margou, Qiemo Country, Xinjiang, China.

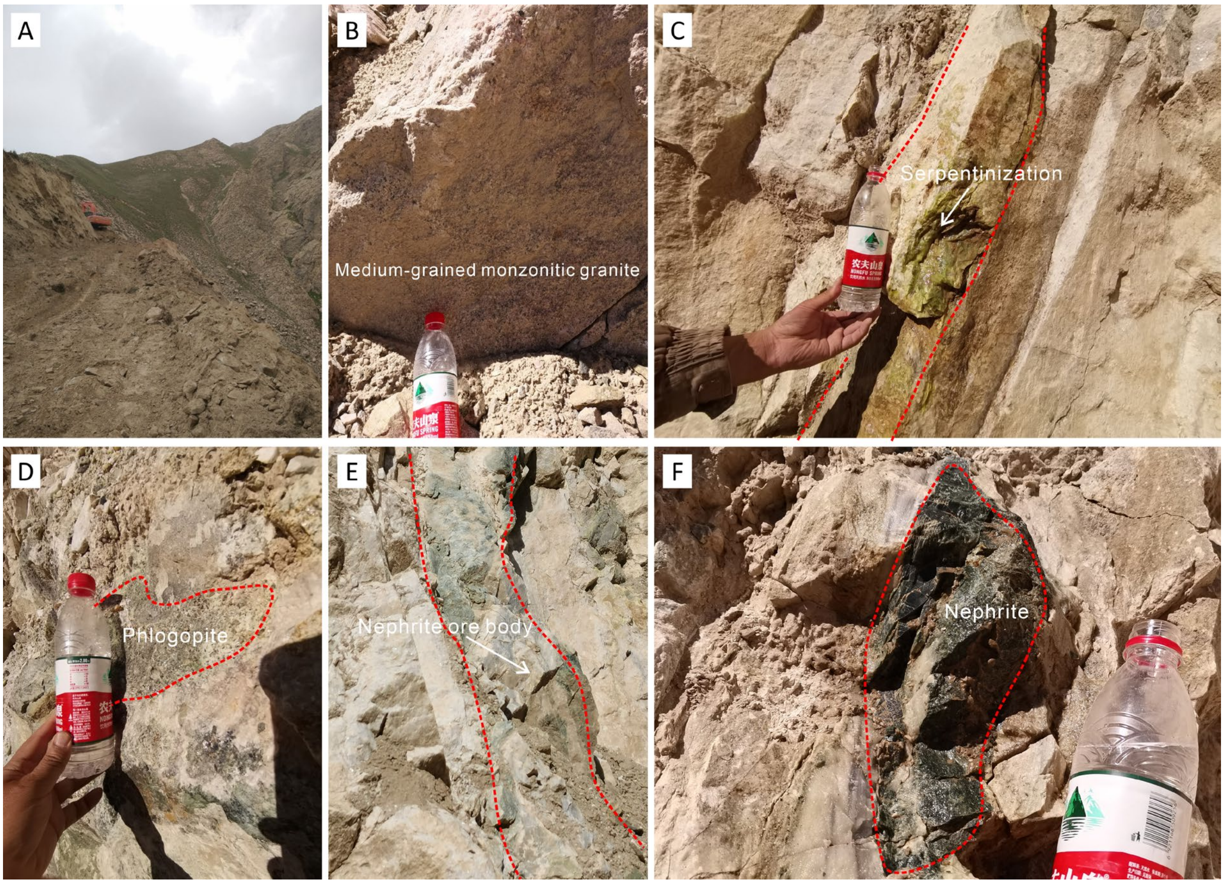


**Figure 3.** (**A**) Field photographs of the Margou nephrite mine. (**B**) Medium-grained monzonitic granite. (**C**) Serpentinization. (**D**) Phlogopite. (**E**,**F**) Margou nephrite.

The ore body, oriented nearly north–south, has a thickness ranging from 1 to 4 m and extends for 25 m. It exhibits a lenticular shape, with a thicker middle section that thins and then disappears at the two ends towards the north and south. After reaching a depth of 15 m, the ore body gradually pinches out. In the vertical section, the magmatic hydrothermal fluid gave rise to a substantial ore body near the contact zone with dolomite marble, subsequently migrating along the marble layer to form three distinct branches.

Tremolite is primarily found forming along the outer contact zone of the marble, which is closely associated with mineralization. Serpentine formation can be observed both in the outer contact zone and the altered marble bedding zone (Figure 3C). Phlogopite occurs in close proximity to the contact zone and the diorite vein (Figure 3D). The diorite vein commonly exhibits disseminated and agglomerated pyrite alteration.

Black cyan nephrite ore occurs in the form of large blocks, with approximately 30% of the texture exhibiting delicacy and high quality (Figure 3E,F). This observation underscores the distinctive geological characteristics and promising quality of the ore at the Margou nephrite mine.

*2.2. Materials*

This article presents a comprehensive examination of the mineralogical and geochemical characteristics of Margou nephrite samples from the Qiemo Formation in the Qiemo area, Xinjiang, China. The nephrite metallogenic belt in the Xinjiang region is primarily distributed in three areas: Shache–Yecheng, Hetian–Yutian, and Qiemo–Ruoqiang. Despite variations in deposit types, all nephrite deposits share similar geological backgrounds, predominantly occurring within the contact zones between Pre-Cambrian dolomitic marble and medium-acidic magmatite [11,20]. The samples investigated in this study come from the Qiemo area, characterized by a consistent distribution of black and black cyan tones.

They exhibit an overall glossy appearance, greasy luster, blocky structure, dense texture, and minimal fissures.

The samples were obtained through in situ extraction of nephrite material at the mining site. Three substantial fragments, exhibiting hues ranging from dark green to black, were earmarked for analytical evaluation. For illustration, the sample identifier "21-A1-1" signifies a specimen collected in 2021 from the mine site ("21"), representing the initial specimen ("1") evaluated at the first analysis location ("A1"). Moreover, the acronym "MY" is utilized to denote "black nephrite jade", as per its Mandarin Chinese pinyin transcription. Remarkably, some black samples even bear a resemblance to pure lacquer, as depicted in Figure 4C. The Ultra-Deep Three-Dimensional Microscope image of the surface of the Margou nephrite sample shows the distribution of pyrite and iron hydroxide, with a strong metallic luster, in which the pyrite is intact (Figure 5).

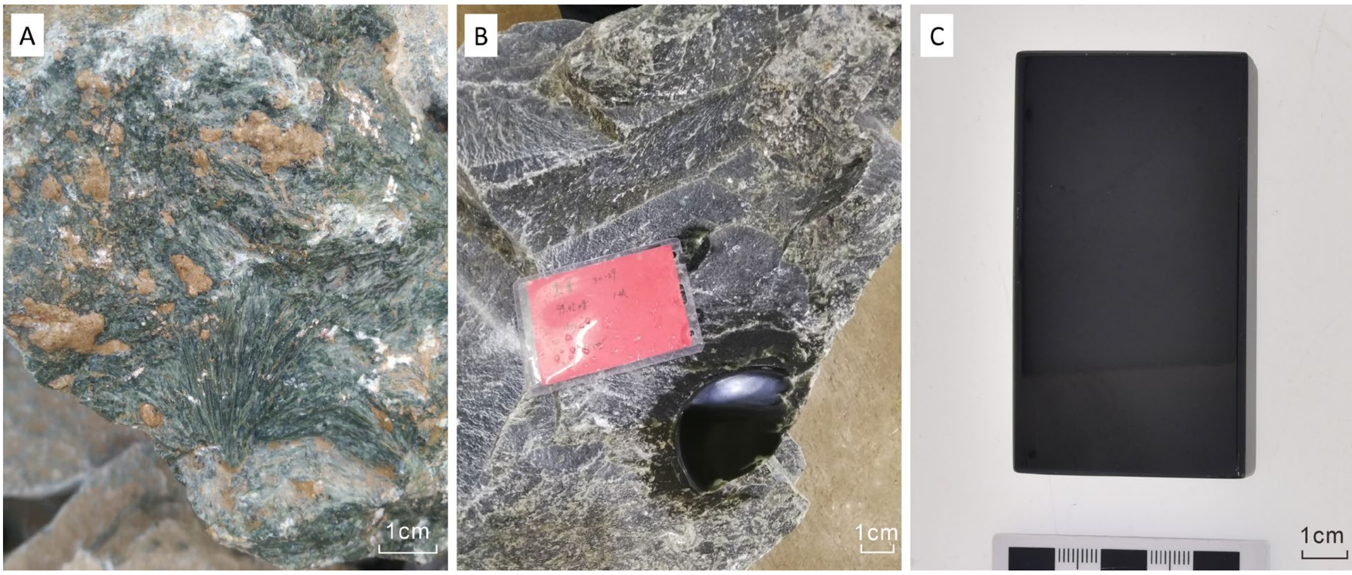


**Figure 4.** Nephrite samples from the Margou nephrite mine in Qiemo Country, Xinjiang, China. (**A**) Picture of a sample of Margou nephrite. (**B**) Picture of a sample of partially polished Margou nephrite sections. (**C**) Picture of a sample of polished Margou nephrite.

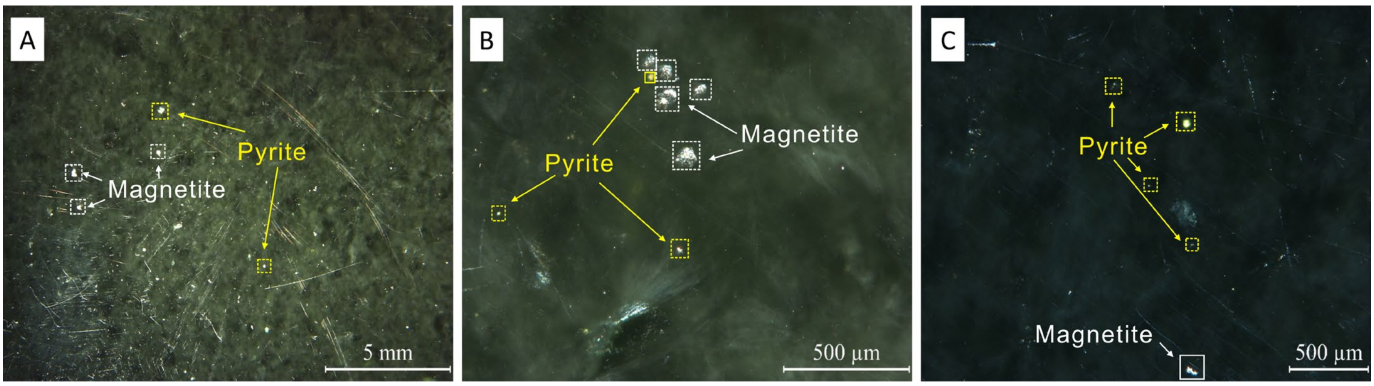


**Figure 5.** (**A**–**C**) Optical images of Margou nephrite sample.

## 3. Methods

(1) Ultra-Deep Three-Dimensional Microscope: The Gemmological Institute at the China University of Geosciences in Wuhan has employed the Leica M205A, an advanced Ultra-Deep Three-Dimensional Microscope, for the meticulous examination and documentation of microscopic features and surface mineralogy of various samples.

(2) Polarizing microscope: Sample observations under both orthogonal and single-polarized light were conducted using an Olimpus BX51 polarizing microscope in the laboratory of Nanjing Shunke Testing Technology Co., Ltd.

(3) Major Elemental Composition Analysis: In order to determine the elemental composition and content of major minerals and accessory minerals in the Margou black and black cyan nephrite, samples were analyzed using a JXA-8230 of JEOL electron probe for microanalysis at Wuhan SampleSolution Analytical Technology Co., Ltd., Wuhan, China. Back-scattered electron (BSE) images and mineral components were obtained using a JSM-IT500 of JEOL InTouchScope series Scanning Electron Microscope at the Institute of Mineral Resources, Chinese Academy of Geological Sciences. The test conditions for these analyses included a voltage of 15 kV, a current of 20 mA, and spot 5 μm. Standard minerals—both natural and artificial—were employed for calibration, and the ZAF correction program provided by the manufacturer was utilized to correct gangue minerals.

(4) Bulk-Rock Major and Trace Element Testing: Bulk-rock geochemical analysis was conducted through X-ray fluorescence at the ALS Minerals Laboratory, Guangzhou. The procedure involved mixing 0.7 g of powdered bulk-rock samples with 5.3 g of $Li_2B_4O_7$, 0.4 g of LiF, and 0.3 g of $NH_4NO_3$ in a 25 mL porcelain crucible. The resulting powder mixture was transferred to a platinum alloy crucible and 1 mL of LiBr solution was added, followed by drying. The sample was then slowly melted in an automatic flame melting machine. Finally, X-ray fluorescence (XRF) analysis of major elements was carried out in a cold glass, with an analysis error below 2%. For analysis of trace elements, 50 mg of bulk-rock powder was dissolved in 1 mL of pure HF and 0.5 mL of $HNO_3$, dried in 15 mL of Savillex Teflon in a screw-cap capsule at 190 °C for one day, then mixed with 0.5 mL of $HNO_3$ and dried again to ensure complete mixing. After that, the sample was mixed with 5 mL of $HNO_3$, sealed in a 130 °C furnace for 3 h, cooled, transferred to a plastic bottle, and diluted to 50 mL before analysis. The trace elements in the sample solution were analyzed through inductively coupled plasma mass spectrometry (ICP-MS) with an analytical accuracy of 5%.

## 4. Results

### *4.1. Petrological Characteristics*

#### 4.1.1. Mineral Components Characteristics

Using microscopic examination and back-scattered electron imaging, the mineralogical composition was elucidated, revealing tremolite–actinolite as the dominant basis minerals, accompanied by minor minerals such as diopside, epidote, pargasite, apatite, zircon, pyrite, and magnetite. The identified mineral assemblage bears a striking similarity to that of the Hetian nephrite sourced from the Karakashi River in the Hetian region [10].

Microscopic and BSE analyses of the Margou black and black cyan nephrite from Qiemo County, Xinjiang, indicated a predominant composition of fine-grained felted tremolite. The tremolite particles exhibit an exceptionally fine texture, making it difficult to distinguish their contours under the microscope (Figure 6A,B). Furthermore, second-stage tremolite can be observed (Figure 7A), which presents a sequence of formation from gray–white fine-grained tremolite to gray coarse-grained tremolite. The optical characteristics of tremolite of different periods remain fairly consistent, exhibiting a second-order interference color ranging from blue to blue–green under orthogonally crossed polarizers while appearing colorless under a single polarizer. The texture is fibrous cryptocrystalline and microcrystalline, with a semi-directional to directional distribution (Figure 6A). The presence of tremolite with different grain sizes indicates that the formation of the Margou nephrite sample involved multiple stages of hydrothermal metasomatic mineralization. Epidotes are relatively common and are mostly distributed within the tremolite matrix or at the periphery of tremolite particles. The images illustrate that epidotes often underwent replacement by tremolite, exhibiting a metasomatic residual structure (Figure 7B). Apatite appears as elongated columnar crystals with a fracture length of up to 600 μm (Figure 7B).

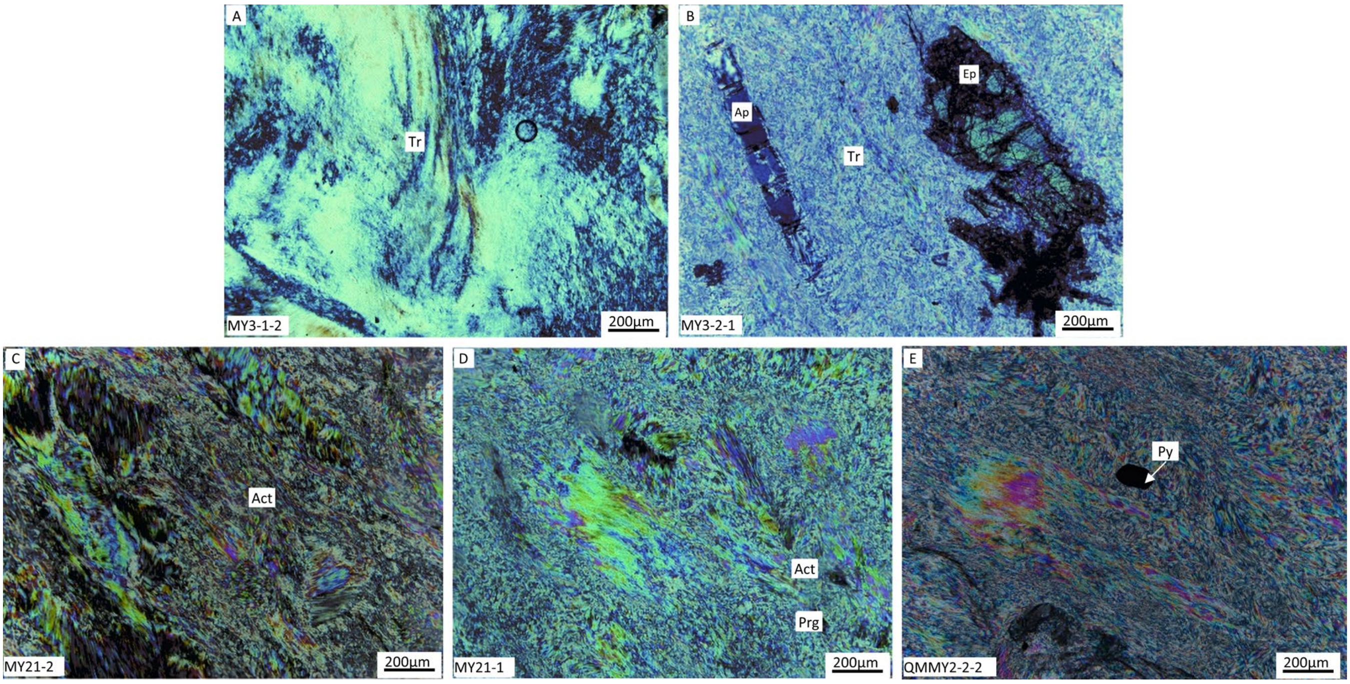


**Figure 6.** Photomicrograph images of Margou nephrite. (**A**) Different periods of tremolite and brownish dissemination. (**B**) Two periods of tremolite, TrI and TrII. (**C**) Distribution of epidote and apatite in fine-grained tremolite aggregates. (**D**) Irregularly outlined epidote and columnar apatite replaced by tremolite. (**E**) The opaque metal mineral is pyrite (Tr, tremolite; Act, actinolite; Prg, pargasite; Ep, epidote; Ap, apatite; Py, pyrite).

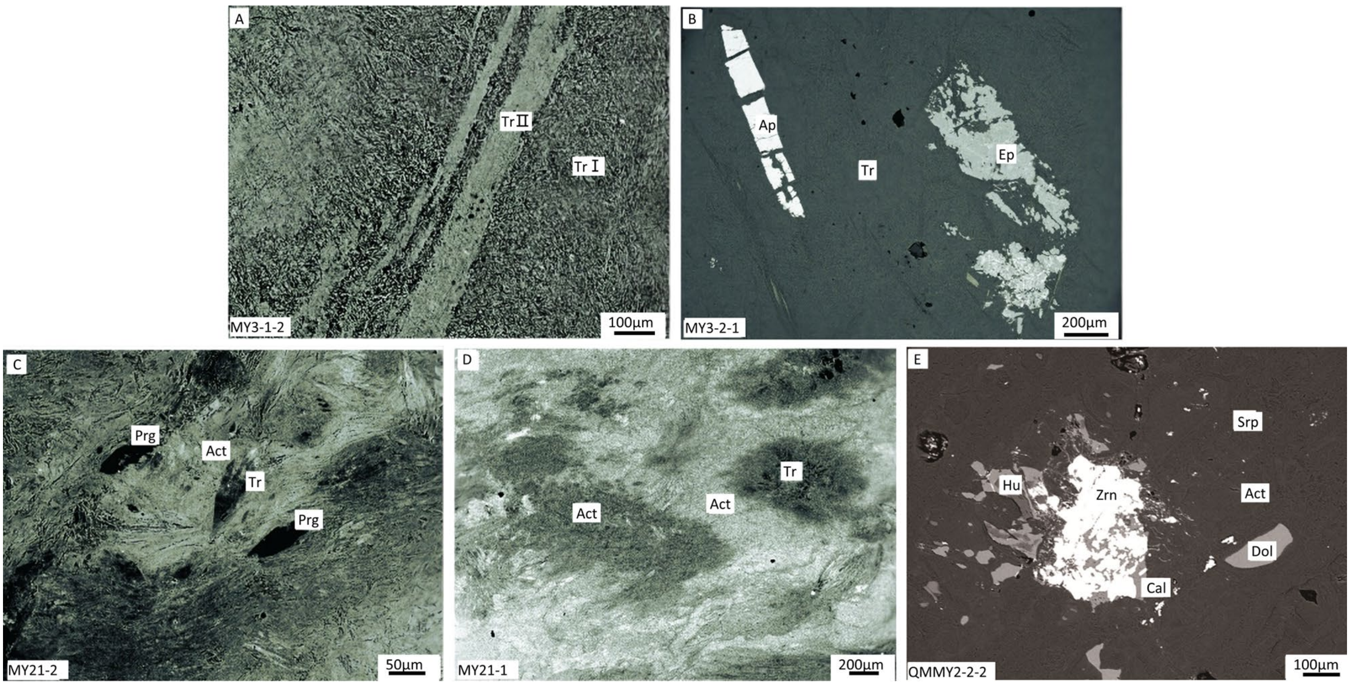


**Figure 7.** Back-scattered electron (BSE) images of Margou nephrite. (**A**) Visible patchy porphyroblastic texture of actinolite and some actinolite fibers arranged in a radial pattern. (**B**) Actinolite replacing tremolite and pargasite. (**C**) Semi-directional to directional distribution of actinolite. (**D**) Tremolite altered by actinolite, exhibiting metasomatic relict texture. (**E**) Zircon and its surrounding minerals (Tr, tremolite; Act, actinolite; Prg, pargasite; Ep, epidote; Ap, apatite; Hu, humite; Zrn, zircon; Srp, serpentine; Dol, dolomite; Cal, calcite).

In the black Margou nephrite, actinolite displays first-order orange and second-order blue–green interference colors, with some actinolite crystals exhibiting a radial arrangement (Figure 6C,D). Coexisting tremolite, actinolite, and pargasite are observed, with actinolite actively replacing tremolite and pargasite, resulting in a metasomatic relict texture for tremolite and pargasite (Figures 6D and 7C). The replacement sequence indicates that the formation of tremolite and pargasite predates that of actinolite. Furthermore, actinolite can also replace tremolite, with tremolite forming a metasomatic relict texture (Figure 7D).

In summary, metasomatism phenomena are prevalent in the Margou black and black cyan nephrite from Qiemo County. The replacement of anhydrous minerals such as diopside and epidote with actinolite and tremolite indicates that the former formed before the latter, in different stages of metamorphic and hydrothermal mineralization. The presence of apatite, zircon (Figure 7E), and other minerals suggests a close association between the formation of the black and black cyan nephrite and granite.

#### 4.1.2. Mineral Chemistry

Electron probe microanalysis was conducted on selected samples of Margou black and black cyan nephrite from Qiemo County, and the specific results are presented in Table 1. The analysis revealed that the main chemical components included $SiO_2$ (56.11–57.90 wt.%), MgO (20.01–24.30 wt.%), and CaO (12.13–14.13 wt.%), with average values of 56.95 wt.%, 21.82 wt.%, and 13.17 wt.%, respectively. Notably, these values were significantly lower than the theoretical value for tremolite (58.18 wt.%, 24.16 wt.%, and 13.18 wt.%, respectively) [21]. According to the nomenclature rules set by the International Mineralogical Association for amphibole, samples with $Mg/(Mg+Fe^{2+}) > 0.9$ are classified as tremolite, whereas those with $Mg/(Mg+Fe^{2+}) < 0.9$ are classified as actinolite. The calculated $Mg/(Mg+Fe^{2+})$ ratios range from 0.86 to 1.0, and the Si and $Mg/(Mg+Fe^{2+})$ binary diagrams confirm the main mineral composition of the black and black cyan nephrite as tremolite–actinolite (Figure 8). For comparison, the composition of $SiO_2$ (43.59–58.46 wt.%), MgO (18.89–26.55 wt.%), and CaO (10.20–23.21 wt.%) in white and green nephrite from the Hetian nephrite of the Alamas marble-type deposit presented overlapping values [20,22,23]. The FeO content exhibited a wide variation (0.08–6.29 wt.%), while the $Cr_2O_3$ content ranged from 0.00 wt.% to 0.04 wt.% and the NiO content varied between 0.00 wt.% and 0.07 wt.%. These values are similar to those typical of magnesian marble-origin tremolite, being notably lower than the values for serpentine-type tremolite of the corresponding type ($Cr_2O_3$ = 0.07–0.43 wt.%, NiO = 0.08–0.36 wt.%) [24].

- Tremolite–Actinolite: Tremolite in the Margou black and black cyan nephrite exhibited 7.73–8.03 a.p.f.u. Si at the T site, 4.43–4.92 a.p.f.u. Mg at the C site, and 1.89–1.96 a.p.f.u. Ca at the B site. These values are slightly lower than those for the Xinjiang Hetian area nephrite sample, with 8.00–8.08 a.p.f.u. Si at the T site, 4.61–4.73 a.p.f.u. Mg at the C site, and 1.88–2.0 a.p.f.u. Ca at the B site. As for the actinolite in Margou black and black cyan nephrite, it showed 7.83–8.01 a.p.f.u. Si at the T site, 4.25–4.62 a.p.f.u. Mg at the C site, and 1.77–1.96 a.p.f.u. Ca at the B site, with Ca exceeding 1.50 a.p.f.u. at the B site. The FeO content ranged from 0.08 wt.% to 6.29 wt.%, higher than that in white nephrite (FeO = 0.07–1.09 wt.%) and green nephrite (FeO = 0.17–4.93 wt.%), but similar to that in Xinjiang black nephrite (FeO = 4.11–14.39 wt.%) and lower than that in Guangxi black nephrite (FeO = 11.67–25.75 wt.%) [24] (Table 2).
- Epidote: In the Margou black and black cyan nephrite from Qiemo County, epidote exhibited a relatively high FeO content (11.43–12.04 wt.%), with $SiO_2$ and CaO contents of 40.72–41.67 wt.% and 23.57–23.69 wt.%, respectively. The atomic composition of each unit of epidote had the following geochemical characteristics (a.p.f.u): Si = 3.15–3.21, Al = 2.05–2.09, and Ca = 1.95–1.96 (Table 2).
- Pargasite: Pargasite in the black nephrite had almost the same composition, with $SiO_2$ content ranging from 46.69 wt.% to 46.73 wt.%, MgO from 20.21 wt.% to 21.18 wt.%, and CaO from 13.80 wt.% to 13.99 wt.%. The atomic composition of each unit

of pargasite had the following geochemical characteristics (a.p.f.u): Si = 6.50–6.53, Al = 1.97–2.12, and Ca = 2.07–2.09 (Table 2).

- Diopside: Diopside commonly exists in magnesian silicate skarn deposits and is considered one of the primary material sources for the formation of Xinjiang nephrite [15,17]. The main chemical components of diopside are $SiO_2$ (54.43–54.49 wt.%), MgO (11.24–17.95 wt.%), and CaO (24.02–26.02 wt.%) (Table 2).

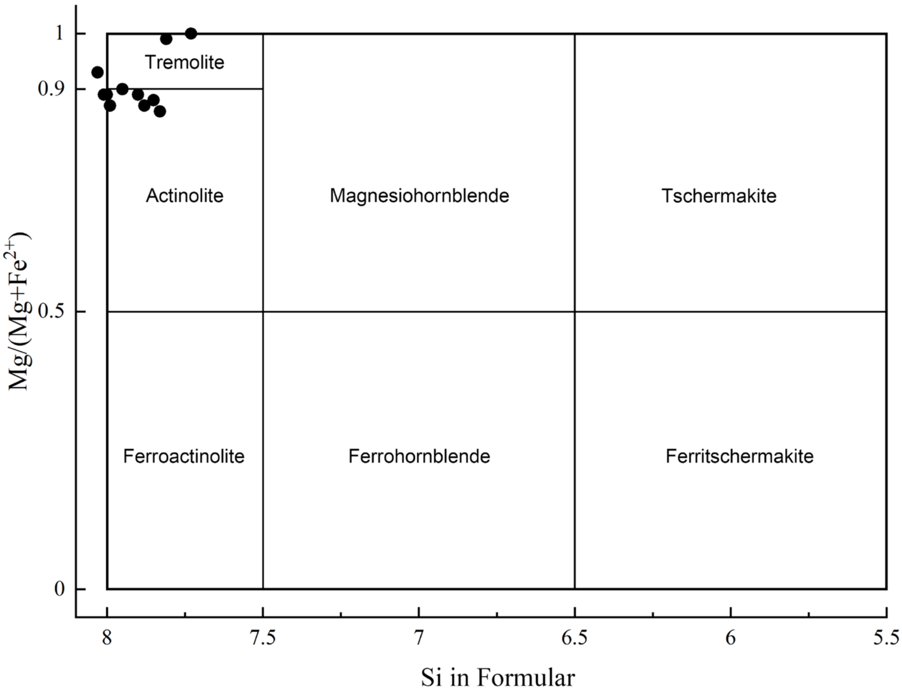


**Figure 8.** Classification diagram of amphibole in Margou nephrite.

**Table 1.** Chemical compositions of main minerals in Margou nephrite determined by EPMA (wt.%).

| Sample No. | 21-1-A1 | 21-1-A2 | 21-1-A3 | 21-1-A4 | 21-2-A1 | 21-2-A2 | 21-2-A3 | 21-2-A4 | 21-3-A1 | 21-3-A2 | 21-3-A3 |
|---|---|---|---|---|---|---|---|---|---|---|---|
| $SiO_2$ | 57.67 | 56.68 | 56.54 | 57.74 | 57.9 | 56.71 | 56.11 | 56.41 | 57.28 | 56.51 | 56.86 |
| $TiO_2$ | 0.03 | 0.00 | 0.00 | 0.03 | 0.00 | 0.03 | 0.00 | 0.08 | 0.00 | 0.00 | 0.00 |
| $Al_2O_3$ | 1.99 | 2.18 | 0.59 | 0.20 | 0.83 | 0.41 | 0.40 | 0.65 | 0.64 | 0.54 | 0.36 |
| $Cr_2O_3$ | 0.02 | 0.04 | 0.00 | 0.00 | 0.00 | 0.00 | 0.00 | 0.03 | 0.03 | 0.00 | 0.00 |
| FeO | 0.43 | 0.17 | 5.56 | 3.03 | 4.29 | 4.91 | 5.29 | 6.29 | 5.26 | 4.71 | 4.66 |
| MnO | 0.00 | 0.06 | 0.14 | 0.02 | 0.20 | 0.20 | 0.23 | 0.22 | 0.05 | 0.08 | 0.10 |
| MgO | 23.44 | 24.30 | 21.21 | 21.53 | 21.63 | 22.06 | 20.01 | 21.05 | 22.58 | 21.03 | 21.14 |
| CaO | 14.13 | 13.85 | 13.38 | 13.77 | 13.1 | 12.73 | 13.05 | 13.55 | 12.82 | 12.13 | 12.4 |
| $Na_2O$ | 0.21 | 0.14 | 0.11 | 0.05 | 0.13 | 0.10 | 0.07 | 0.13 | 0.15 | 0.13 | 0.12 |
| $K_2O$ | 0.02 | 0.00 | 0.04 | 0.04 | 0.04 | 0.04 | 0.06 | 0.06 | 0.06 | 0.07 | 0.05 |
| $P_2O_5$ | 0.01 | 0.02 | 0.01 | 0.03 | 0.03 | 0.00 | 0.03 | 0.00 | 0.01 | 0.00 | 0.09 |
| BaO | 0.00 | 0.00 | 0.02 | 0.03 | 0.02 | 0.01 | 0.00 | 0.06 | 0.04 | 0.04 | 0.00 |
| NiO | 0.06 | 0.00 | 0.07 | 0.00 | 0.00 | 0.00 | 0.00 | 0.00 | 0.00 | 0.00 | 0.00 |
| F | 0.68 | 0.80 | 0.65 | 0.31 | 0.00 | 0.09 | 0.00 | 0.42 | 0.69 | 0.51 | 0.19 |
| Cl | 0.02 | 0.01 | 0.01 | 0.01 | 0.01 | 0.02 | 0.00 | 0.01 | 0.01 | 0.01 | 0.02 |
| Total | 98.72 | 98.25 | 98.31 | 96.77 | 98.17 | 97.30 | 95.25 | 98.96 | 99.62 | 97.75 | 96.24 |
| T-Si | 7.81 | 7.73 | 7.88 | 8.03 | 7.95 | 7.90 | 7.99 | 7.83 | 7.85 | 8.00 | 8.01 |
| T-Al | 0.19 | 0.27 | 0.10 | 0.00 | 0.05 | 0.07 | 0.01 | 0.11 | 0.10 | 0.00 | 0.00 |
| Sum-T | 8.00 | 8.00 | 7.98 | 8.03 | 8.00 | 7.97 | 8.00 | 7.94 | 7.95 | 8.00 | 8.01 |
| C-Al | 0.13 | 0.08 | 0.00 | 0.03 | 0.09 | 0.00 | 0.06 | 0.00 | 0.00 | 0.09 | 0.06 |
| C-Cr | 0.00 | 0.00 | 0.00 | 0.00 | 0.00 | 0.0 | 0.00 | 0.00 | 0.00 | 0.00 | 0.00 |
| C-Mg | 4.73 | 4.92 | 4.41 | 4.46 | 4.43 | 4.58 | 4.25 | 4.36 | 4.62 | 4.44 | 4.44 |
| C-$Fe^{2+}$ | 0.05 | 0.00 | 0.59 | 0.35 | 0.48 | 0.42 | 0.63 | 0.64 | 0.38 | 0.47 | 0.50 |
| C-$Ti^{4+}$ | 0.00 | 0.00 | 0.00 | 0.00 | 0.00 | 0.00 | 0.00 | 0.01 | 0.00 | 0.00 | 0.00 |
| C-$Mn^{2+}$ | 0.00 | 0.00 | 0.00 | 0.00 | 0.00 | 0.00 | 0.03 | 0.00 | 0.00 | 0.00 | 0.00 |
| C-Ca | 0.09 | 0.00 | 0.00 | 0.16 | 0.00 | 0.00 | 0.03 | 0.00 | 0.00 | 0.00 | 0.00 |
| Sum-C | 5.00 | 5.00 | 5.00 | 5.00 | 5.00 | 5.00 | 5.00 | 5.01 | 5.00 | 5.00 | 5.00 |
| B-Mg | 0.00 | 0.02 | 0.00 | 0.00 | 0.00 | 0.00 | 0.00 | 0.00 | 0.00 | 0.00 | 0.00 |
| B-$Fe^{2+}$ | 0.00 | 0.02 | 0.06 | 0.00 | 0.01 | 0.15 | 0.00 | 0.09 | 0.22 | 0.09 | 0.05 |
| B-Mn | 0.00 | 0.01 | 0.02 | 0.00 | 0.02 | 0.02 | 0.00 | 0.03 | 0.01 | 0.01 | 0.01 |
| B-Ca | 1.96 | 1.95 | 1.92 | 1.89 | 1.93 | 1.83 | 1.96 | 1.88 | 1.77 | 1.84 | 1.87 |
| B-Na | 0.04 | 0.00 | 0.00 | 0.01 | 0.04 | 0.00 | 0.02 | 0.00 | 0.00 | 0.04 | 0.03 |
| B-K | 0.00 | 0.00 | 0.00 | 0.01 | 0.01 | 0.00 | 0.01 | 0.00 | 0.00 | 0.01 | 0.01 |
| Sum-B | 2.00 | 2.00 | 2.00 | 1.91 | 2.00 | 2.00 | 1.99 | 2.00 | 2.00 | 1.99 | 1.97 |
| A-Ca | 0.00 | 0.07 | 0.08 | 0.00 | 0.00 | 0.09 | 0.00 | 0.13 | 0.11 | 0.00 | 0.00 |
| A-Na | 0.02 | 0.04 | 0.03 | 0.00 | 0.00 | 0.03 | 0.00 | 0.04 | 0.04 | 0.00 | 0.00 |

**Table 1.** *Cont.*

| Sample No. | 21-1-A1 | 21-1-A2 | 21-1-A3 | 21-1-A4 | 21-2-A1 | 21-2-A2 | 21-2-A3 | 21-2-A4 | 21-3-A1 | 21-3-A2 | 21-3-A3 |
|---|---|---|---|---|---|---|---|---|---|---|---|
| A-K | 0.00 | 0.00 | 0.01 | 0.00 | 0.00 | 0.01 | 0.00 | 0.01 | 0.01 | 0.00 | 0.00 |
| Sum-A | 0.02 | 0.11 | 0.12 | 0.00 | 0.00 | 0.12 | 0.00 | 0.18 | 0.16 | 0.00 | 0.00 |
| Sum-Cat | 15.02 | 15.11 | 15.10 | 14.94 | 15.00 | 15.09 | 14.99 | 15.13 | 15.11 | 14.99 | 14.98 |
| $Mg/(Mg+Fe^{2+})$ | 0.99 | 1.00 | 0.87 | 0.93 | 0.90 | 0.89 | 0.87 | 0.86 | 0.88 | 0.89 | 0.89 |
| Mineral | Tremolite | Tremolite | Actinolite | Tremolite | Tremolite | Actinolite | Actinolite | Actinolite | Actinolite | Actinolite | Actinolite |
| Nephrite Name | Black-Cyan Nephrite | Black-Cyan Nephrite | Black-Cyan Nephrite | Black-Cyan Nephrite | Black-Cyan Nephrite | Black-Cyan Nephrite | Black-Cyan Nephrite | Black-Cyan Nephrite | Black-Cyan Nephrite | Black-Cyan Nephrite | Black-Cyan Nephrite |

Note: Amphibole formulae were re-calculated on the basis of 23 oxygen atoms; 0.00—concentration below the detection limit. T, C, B, and A represent the occupation of cations in tremolite and actinolite.

**Table 2.** Chemical compositions of trace minerals in Margou nephrite determined by EPMA (wt.%).

| Sample No. | 21-1-1A1 | 21-1-1A2 | 21-1-2A3 | 3-2-1-1C | 3-2-1-2A | 3-2-1-2B | 3-1-2-3A | 21-2-1A1 | 3-1-2-3B |
|---|---|---|---|---|---|---|---|---|---|
| $SiO_2$ | 46.69 | 46.73 | 54.49 | 54.43 | 41.67 | 40.72 | 0.09 | 27.98 | 0.16 |
| $TiO_2$ | 0.74 | 0.65 | 0.00 | 0.00 | 0.00 | 0.05 | 0.00 | 0.00 | 0.00 |
| $Al_2O_3$ | 12.93 | 11.97 | 0.28 | 0.50 | 22.58 | 22.92 | 0.00 | 15.32 | 0.02 |
| $Cr_2O_3$ | 0.00 | 0.03 | 0.00 | 0.00 | 0.01 | 0.02 | 0.00 | 0.05 | 0.05 |
| FeO | 0.36 | 0.39 | 0.13 | 4.96 | 11.43 | 12.04 | 0.08 | 14.39 | 55.52 |
| MnO | 0.00 | 0.03 | 0.06 | 2.99 | 0.15 | 0.20 | 0.00 | 0.37 | 0.24 |
| MgO | 20.21 | 21.18 | 17.95 | 11.24 | 0.28 | 0.14 | 0.03 | 21.74 | 0.01 |
| CaO | 13.99 | 13.8 | 26.02 | 24.02 | 23.69 | 23.57 | 54.93 | 0.30 | 0.03 |
| $Na_2O$ | 2.22 | 2.10 | 0.00 | 0.11 | 0.00 | 0.03 | 0.00 | 0.01 | 0.00 |
| $K_2O$ | 0.32 | 0.27 | 0.01 | 0.00 | 0.01 | 0.00 | 0.00 | 0.02 | 0.00 |
| $P_2O_5$ | 0.00 | 0.00 | 0.00 | 0.00 | 0.00 | 0.00 | 41.19 | 0.00 | 0.00 |
| F | 0.63 | 0.93 | 0.00 | 0.00 | 0.00 | 0.00 | 3.36 | 0.21 | 0.00 |
| Total | 98.13 | 98.20 | 99.12 | 100.38 | 99.87 | 99.71 | 99.85 | 80.52 | 56.03 |
| Si | 6.50 | 6.53 | 1.99 | 2.09 | 3.21 | 3.15 | 0.01 | 3.07 | - |
| Ti | 0.08 | 0.07 | 0.00 | 0.00 | 0.00 | 0.00 | 0.00 | 0.00 | - |
| Al | 2.12 | 1.97 | 0.01 | 0.02 | 2.05 | 2.09 | 0.00 | 1.98 | - |
| Cr | 0.00 | 0.00 | 0.00 | 0.00 | 0.00 | 0.00 | 0.00 | 0.00 | - |
| $Fe^{2+}$ | 0.04 | 0.05 | 0.00 | 0.16 | 0.74 | 0.78 | 0.01 | 1.32 | - |
| Mn | 0.00 | 0.00 | 0.00 | 0.10 | 0.01 | 0.01 | 0.00 | 0.03 | - |
| Mg | 4.20 | 4.41 | 0.98 | 0.64 | 0.03 | 0.02 | 0.00 | 3.55 | - |
| Ca | 2.09 | 2.07 | 1.02 | 0.99 | 1.96 | 1.95 | 5.01 | 0.04 | - |
| Na | 0.60 | 0.57 | 0.00 | 0.01 | 0.00 | 0.00 | 0.00 | 0.00 | - |
| K | 0.06 | 0.05 | 0.00 | 0.00 | 0.00 | 0.00 | 0.00 | 0.00 | - |
| P | 0.00 | 0.00 | 0.00 | 0.00 | 0.00 | 0.00 | 2.97 | 0.00 | - |
| Total | 15.69 | 15.72 | 4.00 | 4.00 | 7.99 | 8.00 | 8.00 | 9.90 | - |
| Mineral | Pargasite | Pargasite | Diopside | Diopside | Epidote | Epidote | Apatite | Chlorite | Ferric hydroxide |

Note: Amphibole formulae were re-calculated on the basis of 23 oxygen atoms; 0.00—concentration below the detection limit.

### *4.2. Bulk-Rock Major and Trace Elements*

The results of the major element analyses obtained by XRF (Table 3) indicated a generally homogeneous chemical composition for the Margou black and black cyan nephrite, with relatively stable component contents. The $SiO_2$ content ranges from 56.38 wt.% to 56.91 wt.%, MgO content from 21.3 wt.% to 22.20 wt.%, and CaO content from 13.10 wt.% to 13.45 wt.%. These values overlap with the chemical composition of black nephrite from the Yulong Kashgar River and Karakashi River, with $SiO_2$ content ranging from 51.09 wt.% to 57.01 wt.%, MgO content from 14.24 wt.% to 24.80 wt.%, and CaO content from 10.86 wt.% to 13.88 wt.% [18]. The average values of Margou nephrites for $SiO_2$, CaO, and MgO were 56.65 wt.%, 13.25 wt.%, and 21.8 wt.%, respectively. Importantly, these values are significantly higher than those of actinolite ($SiO_2$ = 53 wt.%; CaO = 13.80 wt.%; MgO = 14.42 wt.%) [20]. Previous studies have suggested that, with an increase in FeO content in nephrite, amphibole changes its composition from tremolite through actinolite to ferro-actinolite [8]. In the Xinjiang Qiemo Margou black and black cyan nephrite, the main mineral was tremolite, with FeO content in the bulk-rock chemical composition ranging from 3.97 wt.% to 5.09 wt.%, and $TFe_2O_3$ content ranging from 4.68 wt.% to 6.11 wt.%. These values overlap with the content of FeO (0.48–9.55 wt.%) and $TFe_2O_3$ (0.56–16.23 wt.%) in black nephrite from the Karakashi River, some of the black nephrite samples with low FeO contents (0.52 wt.%, 0.56 wt.%, and 0.48 wt.%, respectively) appear black because of the presence of large amounts of graphite [18]. Table 4 provides a comparison of the chemical composition of the nephrite considered in this study and that of samples from other nephrite mines in Xinjiang.

**Table 3.** XRF analyses of major elements in Margou black and black cyan nephrite from Qiemo Xinjiang.

| Sample | Content (wt.%) | | |
|---|---|---|---|
| | MY 2021-3-1 | MY 2021-3-2 | MY 2021-3-3 |
| $SiO_2$ | 56.65 | 56.38 | 56.91 |
| $Al_2O_3$ | 0.62 | 0.89 | 0.53 |
| CaO | 13.10 | 13.20 | 13.45 |
| $TFe_2O_3$ | 5.40 | 6.11 | 4.68 |
| FeO | 4.54 | 5.09 | 3.97 |
| $K_2O$ | 0.08 | 0.08 | 0.05 |
| MgO | 21.90 | 21.30 | 22.20 |
| MnO | 0.28 | 0.33 | 0.30 |
| $Na_2O$ | 0.05 | 0.04 | 0.05 |
| $TiO_2$ | 0.02 | 0.02 | 0.00 |
| BaO | 0.00 | 0.01 | 0.01 |
| $Cr_2O_3$ | 0.01 | 0.01 | 0.00 |
| LOI | 2.52 | 2.44 | 2.75 |
| Total | 105.17 | 105.90 | 104.90 |

Note: T—total; LOI—loss on ignition.

**Table 4.** Chemical compositions of nephrite samples from Xinjiang.

| Chemical Composition | Content | Margou | Other Deposits in Xinjiang | |
|---|---|---|---|---|
| | | Average | Black Placer Nephrites from Yurungkash and Karakash Rivers [18] | Green Nephrites from Alamas [20–24] |
| $SiO_2$ | wt.% | 56.65 | 55.03 | 57.41 |
| MgO | | 21.80 | 22.20 | 25.17 |
| CaO | | 13.25 | 12.36 | 12.21 |
| FeO | | 4.35 | 2.29 | 1.13 |
| $TFe_2O_3$ | | 5.40 | 3.74 | 1.43 |
| Total | | 101.45 | 95.62 | 97.35 |
| Cr | μg/g | 13.67 | 9.89 | 120.32 |
| Ni | | 3.50 | 16.83 | 2.03 |

Trace element analyses were conducted on the black and black cyan nephrite, the detailed results of which are presented in Table 5. Crucial elements in nephrite genesis, such as Cr, Ni, and Co, were examined, which are commonly utilized to classify the nephrite genesis type [7,22]. In the Xinjiang Qiemo Margou black and black cyan nephrite, the Cr and Ni content ranges are 6–21 μg/g and 2.5–4.5 μg/g, respectively. These values overlap with those of nephrite materials from the Alamas and Hetian placer deposits—namely, Cr (8.95–178.7 μg/g) and Ni (0.05–3.95 μg/g), and Cr (5.44–28.1 μg/g) and Ni (9.44–18.2 μg/g), respectively [20,22,23]. The Cr and Ni contents in black and black cyan nephrite from Qiemo Margou suggest that it can be classified as marble-related Hetian nephrite, showing content comparable to that of dolomitic marble-type nephrite. In this context, Cr ranges from 2 to 29 μg/g and Ni from 0.05 to 471 μg/g. These values are notably lower than the Cr (900–2812 μg/g) and Ni (959–1898 μg/g) [22] contents in serpentinite-type nephrite.

**Table 5.** Bulk-rock trace element composition obtained by XRF of Margou black and black cyan nephrites from Qiemo Xinjiang.

| Sample | Content (μg/g) | | | |
|---|---|---|---|---|
| | **MY 2021-3-1** | **MY 2021-3-2** | **MY 2021-3-3** | **Average** |
| Li | 4.80 | 4.10 | 4.40 | 4.43 |
| Be | 18.2 | 15.05 | 12.90 | 15.38 |
| Cr | 14.00 | 21.00 | 6.00 | 13.67 |
| Co | 34.60 | 36.90 | 30.60 | 34.03 |
| Ni | 3.50 | 4.50 | 2.50 | 3.50 |
| Cu | 4.40 | 4.30 | 2.70 | 3.80 |
| Zn | 105.00 | 127.00 | 135.00 | 122.33 |
| Ga | 1.10 | 1.50 | 1.30 | 1.30 |
| Rb | 5.30 | 4.40 | 1.90 | 3.87 |
| Sr | 7.00 | 20.50 | 6.00 | 11.17 |
| Mo | 2.01 | 1.58 | 0.55 | 1.38 |
| Cd | 0.04 | 0.06 | 0.06 | 0.05 |
| In | 0.006 | 0.007 | 0.069 | 0.03 |
| Cs | 1.75 | 1.93 | 1.06 | 1.58 |
| Ba | 3.70 | 5.70 | <0.50 | 3.13 |
| Ti | 0.01 | 0.02 | <0.01 | 0.01 |
| Pb | 5.30 | 10.30 | 7.60 | 7.73 |
| Bi | 0.03 | 0.04 | 0.03 | 0.03 |
| Th | 0.51 | 1.54 | 0.05 | 0.70 |
| U | 0.52 | 0.69 | 0.29 | 0.50 |
| Nb | 8.60 | 1.70 | 10.30 | 6.87 |
| Ta | 0.20 | <0.05 | 0.76 | 0.32 |
| Zr | 4.00 | 10.00 | <2.00 | 4.67 |
| Hf | 0.10 | 0.30 | <0.10 | 0.13 |
| Sn | 0.40 | 0.50 | 2.30 | 1.07 |
| Sb | 0.23 | 0.16 | 0.33 | 0.24 |
| TI | 0.04 | 0.04 | 0.02 | 0.03 |
| W | 0.80 | 0.20 | 1.20 | 0.73 |
| As | <0.20 | <0.20 | 0.40 | 0.13 |
| V | 11.00 | 14.00 | 11.00 | 12.00 |
| La | 0.10 | 8.00 | <0.10 | 2.70 |
| Ce | 0.10 | 16.50 | <0.10 | 5.53 |
| Pr | 0.03 | 1.96 | <0.02 | 0.66 |
| Nd | 0.10 | 7.80 | 0.10 | 2.67 |
| Sm | 0.05 | 1.41 | 0.03 | 0.50 |
| Eu | <0.02 | 0.07 | <0.02 | 0.02 |
| Gd | 0.09 | 1.02 | 0.08 | 0.40 |
| Tb | 0.02 | 0.15 | 0.02 | 0.06 |
| Dy | 0.16 | 0.72 | 0.16 | 0.35 |
| Ho | 0.05 | 0.13 | 0.06 | 0.08 |
| Er | 0.25 | 0.38 | 0.28 | 0.30 |
| Tm | 0.07 | 0.08 | 0.09 | 0.08 |
| Yb | 0.61 | 0.59 | 0.72 | 0.64 |
| Lu | 0.10 | 0.09 | 0.10 | 0.10 |
| Sc | 0.50 | 0.70 | 0.20 | 0.47 |
| Y | 1.90 | 4.00 | 2.6 | 2.83 |
| $\delta$Eu | 0.00 | 0.17 | 0.00 | 0.06 |
| $[La/Yb]_N$ | 0.12 | 9.73 | 0.00 | 3.28 |
| LREE | 0.38 | 35.74 | 0.13 | 12.08 |
| HREE | 1.35 | 3.16 | 1.51 | 2.01 |
| ∑REE | 1.73 | 38.9 | 1.64 | 14.09 |

*4.3. Rare Earth Element (REE) Analysis*

The Margou black and black cyan nephrite samples displayed a negative Eu anomaly (δEu = 0.00–0.17), likely resulting from some degree of fractional crystallization during the mineralization process [19]. This result overlaps with data indicating negative Eu anomalies (δEu = 0.03–0.21) in the Alamas deposit, a typical deposit associated with marble [20,22]. The LREE enrichment (LREE: La–Eu) exhibited a right deviation, while the HREE flatness (HREE: Gd–Lu) presented flat characteristics in Margou black and black cyan nephrite, consistent with the rare earth distribution pattern of Hetian nephrite in the Alamas deposit (Figure 9A). This pattern is similar to that of granite. Furthermore, the ∑REE total abundance in Margou black cyan nephrite was low, ranging from 1.64 to 38.9 µg/g (∑REE average 14.09 µg/g) (Table 5), similar to the content of rare earth elements in magnesian marble-type Hetian nephrite deposits (2.84–84.81 µg/g) [16,23]. This suggests that nephrite formation involves hydrothermal fluids evolving from intrusive pyrolith (granodiorite) and replacing local surrounding rocks [18]. There was a significant depletion of Ti, and a lack of Ba and Th; however, high-field-strength elements (Zr, Hf, and Nb) were high or almost not depleted (Figure 9B), resembling the rare earth elements characteristic of black nephrite samples from the Karakashi River.

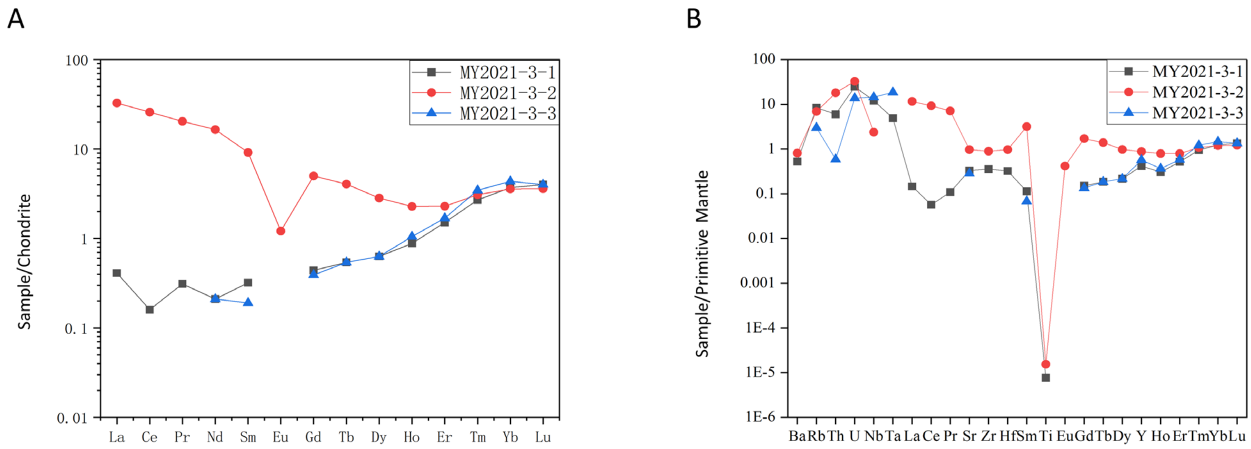


**Figure 9.** (**A**) Rare earth element distribution curve of Qiemo black and black cyan nephrite in Xinjiang. (**B**) Spider diagram of trace elements in Qiemo black and black cyan nephrite in Xinjiang (digitized standard value data: Sun and McDonough, 1989).

Previous studies have indicated that the magmatic rocks in magnesian marble-type skarn Hetian nephrite deposits show high rare earth element contents, Eu-negative anomalies, an LREE right deviation, and an HREE flat rare earth distribution pattern, while magnesian marble is characterized by a relatively stable rare earth distribution pattern and low rare earth content [25]. The REE distribution patterns and contents in the black cyan and black nephrite of Qiemo Margou show that these nephrites mainly inherited the geochemical characteristics of the surrounding magmatic rocks and magnesium marble, indicating that the Qiemo Margou black and black cyan nephrites belong to the magnesian marble skarn-type Xinjiang nephrite deposit.

## 5. Discussion

*5.1. Genetic Types of Qiemo Margou Black Cyan and Black Nephrite*

In general, Cr, Ni, and Co are crucial elements in nephrite formation processes, and are commonly analyzed for their identification [7]. In particular, Cr, Ni, and Co elements can be used to distinguish nephrite associated with dolomite marble from that associated with serpentinite [26]. Serpentinite-type nephrite exhibits higher bulk-rock concentrations of Cr (900–2812 µg/g), Ni (959–1898 µg/g), and Co (42–207 µg/g), while dolomite marble-type nephrite presents lower concentrations of Cr (2–79 µg/g), Ni (0.05–471 µg/g), and Co (0.5–10 µg/g). The bulk-rock trace element analysis in the Qiemo Margou black and black cyan nephrite revealed Cr and Ni concentrations of 6–21 μg/g and 2.5–4.5 μg/g, respectively, consistent with other dolomite marble-type nephrite and significantly lower than those in serpentinite-type nephrite, indicating that the Qiemo Margou black and black cyan nephrite can be classified as a marble-related nephrite.

Bulk-rock analysis of rare earth elements in the Qiemo Margou black and black cyan nephrite highlighted its similarities with magnesian dolomite marble-type nephrite. The Rare Earth distribution pattern curve of Qiemo Margou black cyan nephrite showed a negative Eu anomaly (δEu = 0.00–0.17), a decrease in LREE, and a flat HREE, with low total REE abundance, ranging from 1.64 to 38.9 μg/g (average ∑REE = 14.09 μg/g). The rare earth element distribution pattern and contents in Qiemo Margou black and black cyan nephrite mainly reveal that it inherited the geochemical characteristics of magmatic rocks and marble rocks, indicating that the Qiemo Margou black and black cyan nephrites belong to the magnesian marble-type skarn nephrite deposit.

### *5.2. Coloration Factors of Black Cyan and Black Qiemo Margou Nephrite*

Color represents a crucial criterion not only for evaluating the quality of nephrites but also for their classification [19]. Based on its color, nephrite shows about seven types: white nephrite, bluish-white nephrite, green nephrite jade, black nephrite, brown nephrite, yellow nephrite, and green nephrite jade. In particular, black nephrite is characterized by its primary mineral components, which include tremolite, actinolite, and ferro-actinolite [10].

Summarizing the findings from prior research, four potential factors influencing the coloration of black nephrite have been identified: (1) High graphite content. Despite a low $Fe_2O_3$ content ($TFe_2O_3$: 0.56–4.74 wt.%) [27] in a sample, a high graphite content can generate an overall black color [28]. (2) Some samples exhibit high $TFe_2O_3$ content (>17wt.%), and the Fe elements appear as $Fe(OH)_3$ in a vein-like pattern in nephrite, leading to increased density and a darker black color [29]. (3) Samples primarily composed of darker green tremolite are coupled with varying quantities of Fe (FeO = 0.48–9.55 wt.%), which contributes to a specific type of black coloration [29]. (4) Samples predominantly composed of actinolite or ferro-actinolite, with higher Fe content (FeO = 11.67–25.75 wt.%), produce an overall black color [24,29,30].

A previous study has reported that the color of nephrite can be differentiated based on the w(FeO) content, indicating a connection between nephrite color and Fe content. The color-causing element Fe in the tremolite structure of nephrite mainly originates from granite, which typically lacks Cr and Ni in the tremolite crystal structure [29]. The Qiemo Margou black cyan and black nephrite show relatively high FeO (3.97–5.09wt.%) and $TFe_2O_3$ (4.68–6.11wt.%) contents. For comparison, the FeO content of Gobi nephrite is between 0.36 and 1.83 wt.% [6,31], that of Alamas white nephrite and of green nephrite is between 0.41 wt.% and 1.96 wt.% [3], that of Karakax River green nephrite is between 0.67 wt.% and 3.18 wt.%, and that of black nephrite is between 0.48 wt.% and 9.55 wt.%. White nephrite has $TFe_2O_3$ content ranging from 0.33 wt.% to 1.42 wt.%, bluish-white nephrite has $TFe_2O_3$ content ranging from 0.43 wt.% to 0.96 wt.%, and green nephrite has $TFe_2O_3$ content ranging from 0.77 wt.% to 3.97 wt.%. The $TFe_2O_3$ content of green nephrite ranges between 0.77 wt.% and 3.97 wt.%, and that of black nephrite from the Xinjiang Kalakash River is between 0.56 wt.% and 16.23 wt.%. Overall, the FeO and $TFe_2O_3$ contents of the Qiemo Margou black cyan and black nephrite samples are close to those of black nephrite from the Karakax River. Furthermore, the contents of Cr and Ni in the Qiemo Margou black cyan and black nephrite samples are irregular and consistently below 25 μg/g and 5 μg/g, respectively, lower than those in dolomite marble-type nephrite [29], as well as white to bluish-white nephrite from the Xinjiang Hetian area. These data and the limited presence of graphite in the samples demonstrate that the black cyan color of Margou and the black color of Qiemo nephrite can be attributed to higher iron content. The color also does not appear to be related to the Cr and Ni contents.

## 6. Conclusions

This paper provided insights into the mineralogical and chemical composition of Qiemo Margou black and black cyan nephrite. The obtained results revealed that the considered nephrite samples are predominantly composed of tremolite–actinolite, with minor minerals such as diopside, epidote, pargasite, apatite, zircon, pyrite, and magnetite. The comparison of the concentrations of Cr and Ni and of the rare earth elements with the composition of other nephrite samples allowed us to conclude that the Qiemo Margou black cyan and black nephrite can be considered to be typical magnesian skarn-type nephrite. The geochemical characteristics of these nephrite samples are consistent with those of Yutian nephrite, Pishan brown nephrite, and the White Jade River and Black Jade River material deposits, indicating that the material sources and deposit types of Qiemo Margou black and black cyan nephrite are consistent with the deposits in these areas. Margou nephrite presents black cyan and black colors due to its high iron content.

**Author Contributions:** Conceptualization and methodology, T.F. and M.Y.; experiment, T.F.; software, T.F. and Y.C.; formal analysis, T.F.; writing—original draft preparation, T.F.; writing—review and editing, T.F. and Y.C.; project administration, M.Y. All authors have read and agreed to the published version of the manuscript.

**Funding:** This research was funded by the Gemmological Institute Center of China University of Geosciences (Wuhan), grant number: CIGTXM-04-S202145. Furthermore, support was received through a grant provided by the Major Programs of the National Cultural Heritage Administration of China for investigating civilizational processes in the middle reaches of the Yangtze River during the Xia, Shang, and Zhou periods (Heritage Protection Letter (2020) No. 444).

**Data Availability Statement:** The data supporting the reported results can be provided by the corresponding author upon request.

**Acknowledgments:** We express our sincere appreciation to Han Hongwei of Qiemo County Jinshan Jade Crafts Co., Ltd., for providing nephrite samples and deposit photographs. We also extend heartfelt gratitude to the Editors, and the anonymous Reviewers for their invaluable and constructive feedback, which significantly enhanced the quality of the manuscript.

**Conflicts of Interest:** The authors declare no conflicts of interest.

## References

1. Harlow, G.E.; Sorensen, S.S. Jade (Nephrite and Jadeitite) and Serpentinite: Metasomatic Connections. *Int. Geol. Rev.* **2005**, *47*, 113–146. [CrossRef]
2. Liang, H.; Shi, G.; Yuan, Y.; Cao, C.; Sun, X.; Zhang, X. Polysynthetic Twinning of Diopsides in the Niewang and Tatliksu Nephrite Deposits, Xinjiang, China. *Minerals* **2022**, *12*, 1575. [CrossRef]
3. Zhang, X.; Shi, G.; Zhang, X.; Gao, K. Formation of the Nephrite Deposit with Five Mineral Assemblage Zones in the Central Western Kunlun Mountains, China. *J. Petrol.* **2022**, *63*, egac117. [CrossRef]
4. Gao, K.; Shi, G.; Wang, M.; Xie, G.; Wang, J.; Zhang, X.; Fang, T.; Lei, W.; Liu, Y. The Tashisayi Nephrite Deposit from South Altyn Tagh, Xinjiang, Northwest China. *Geosci. Front.* **2019**, *10*, 1597–1612. [CrossRef]
5. Jiang, T.; Shi, G.; Ye, D.; Zhang, X.; Zhang, L.; Han, H. A New Type of White Nephrite from Limestone Replacement along the Kunlun–Altyn Tagh Mountains: A Case from the Mida Deposit, Qiemo County, Xinjiang, China. *Crystals* **2023**, *13*, 1677. [CrossRef]
6. Liu, X.F.; Jia, Y.H.; Liu, Y. Geochemical Characteristics and Genesis Types of Gobi in Ruqiang-Qiemo Xinjian. *Rock Miner. Anal.* **2019**, *38*, 316–325. (In Chinese with English Abstract) [CrossRef]
7. Bai, F.; Li, G.; Lei, J.; Sun, J. Mineralogy, Geochemistry, and Petrogenesis of Nephrite from Panshi, Jilin, Northeast China. *Ore Geol. Rev.* **2019**, *115*, 103171. [CrossRef]
8. Xu, H.; Bai, F.; Jiang, D. Geochemical Characteristics and Composition Changes of Tremolite at Various Stages in the Mineralization Process of Nephrite from Tieli, Heilongjiang, Northeastern China. *Arab. J. Geosci.* **2021**, *14*, 204. [CrossRef]
9. Fang, T.; Wang, S.Q. Discovery and Discussion on Cat's Eye of Qiemo Sugar nephrite in Xinjiang. In Proceedings of the China International Jewelry Academic Exchange Conference, Beijing, China, 13 November 2019; Volume 11, pp. 244–249. (In Chinese with English Abstract) [CrossRef]
10. Zhang, C.; Yang, F.; Yu, X.; Liu, J.; Carranza, E.J.M.; Chi, J.; Zhang, P. Spatial-Temporal Distribution, Metallogenic Mechanisms and Genetic Types of Nephrite Jade Deposits in China. *Front. Earth Sci.* **2023**, *11*, 1047707. [CrossRef]

11. Jing, Y.; Liu, Y. Genesis and Mineralogical Studies of Zircons in the Alamas, Yurungkash, and Karakash Nephrite Deposits, Western Kunlun, Xinjiang, China. *Ore Geol. Rev.* **2022**, *149*, 105087. [CrossRef]
12. Fang, T.; Wang, S.Q. Study on the "silk effect" of transparent gray-purple nephrite. In Proceedings of the China International Jewelry Academic Exchange Conference (2021), Beijing, China, 18–22 November 2021; Volume 1, pp. 216–223. (In Chinese with English Abstract) [CrossRef]
13. Liu, X.; Gil, G.; Liu, Y.; He, X.; Syczewski, M.; Bagiński, B.; Fang, T.; Shu, X. Timing of Formation and Cause of Coloration of Brown Nephrite from the Tiantai Deposit, South Altyn Tagh, Northwestern China. *Ore Geol. Rev.* **2021**, *131*, 103972. [CrossRef]
14. Ling, X.-X.; Schmädicke, E.; Li, Q.-L.; Gose, J.; Wu, R.-H.; Wang, S.-Q.; Liu, Y.; Tang, G.-Q.; Li, X.-H. Age Determination of Nephrite by In-Situ SIMS U–Pb Dating Syngenetic Titanite: A Case Study of the Nephrite Deposit from Luanchuan, Henan, China. *Lithos* **2015**, *220*, 289–299. [CrossRef]
15. Jiang, Y.; Shi, G.; Xu, L.; Li, X. Mineralogy and Geochemistry of Nephrite Jade from Yinggelike Deposit, Altyn Tagh (Xinjiang, NW China). *Minerals* **2020**, *10*, 418. [CrossRef]
16. Liu, Y.; Deng, J.; Shi, G.; Sun, X.; Yang, L. Geochemistry and Petrogenesis of Placer Nephrite from Hetian, Xinjiang, Northwest China. *Ore Geol. Rev.* **2011**, *41*, 122–132. [CrossRef]
17. Zhang, C.; Yu, X.; Yang, F.; Santosh, M.; Huo, D. Petrology and Geochronology of the Yushigou Nephrite Jade from the North Qilian Orogen, NW China: Implications for Subduction-Related Processes. *Lithos* **2021**, *380*, 105894. [CrossRef]
18. Liu, Y.; Zhang, R.-Q.; Abuduwayiti, M.; Wang, C.; Zhang, S.; Shen, C.; Zhang, Z.; He, M.; Zhang, Y.; Yang, X. SHRIMP U–Pb Zircon Ages, Mineral Compositions and Geochemistry of Placer Nephrite in the Yurungkash and Karakash River Deposits, West Kunlun, Xinjiang, Northwest China: Implication for a Magnesium Skarn. *Ore Geol. Rev.* **2016**, *72*, 699–727. [CrossRef]
19. Li, W.W.; Wu, R.H. Study on color and colorimetry of Hetian jade. *Bull. Mineral. Petrol. Geochem.* **1999**, *4*, 418–422. Available online: https://www.cqvip.com/qk/84215x/199904/3000836567.html (accessed on 31 January 2024). (In Chinese with English Abstract)
20. Liu, Y.; Deng, J.; Shi, G.; Yui, T.-F.; Zhang, G.; Abuduwayiti, M.; Yang, L.; Sun, X. Geochemistry and Petrology of Nephrite from Alamas, Xinjiang, NW China. *J. Asian Earth Sci.* **2011**, *42*, 440–451. [CrossRef]
21. Li, N.; Bai, F.; Xu, L.; Che, Y. Geochemical Characteristics and Ore-Forming Mechanism of Luodian Nephrite Deposit, Southwest China and Comparison with Other Nephrite Deposits in Asia. *Ore Geol. Rev.* **2023**, *160*, 105604. [CrossRef]
22. Liu, Y.; Deng, J.; Shi, G.; Lu, T.; He, H.; Ng, Y.; Shen, C.; Yang, L.; Wang, Q. Chemical Zone of Nephrite in Alamas, Xinjiang, China. *Resour. Geol.* **2010**, *60*, 249–259. [CrossRef]
23. Liu, Y.; Zhang, R.; Zhang, Z.; Shi, G.; Zhang, Q.; Abuduwayiti, M.; Liu, J. Mineral Inclusions and SHRIMP U–Pb Dating of Zircons from the Alamas Nephrite and Granodiorite: Implications for the Genesis of a Magnesian Skarn Deposit. *Lithos* **2015**, *212*, 128–144. [CrossRef]
24. Zhong, Q.; Liao, Z.; Qi, L.; Zhou, Z. Black Nephrite Jade from Guangxi, Southern China. *Gems Gemol.* **2019**, *55*, 198–215. [CrossRef]
25. Su, Y.; Yang, M. Combining Rare Earth Element Analysis and Chemometric Method to Determine the Geographical Origin of Nephrite. *Minerals* **2022**, *12*, 1399. [CrossRef]
26. Adamo, I.; Bocchio, R. Nephrite Jade from Val Malenco, Italy: Review and Update. *Gems Gemol.* **2013**, *49*, 98–106. [CrossRef]
27. Zheng, J.; Chen, L.; Zhang, C.; Liu, Y.; Tian, R.; Wu, J.; Wu, Y.; Zhang, S. Constraints on Crystallinity of Graphite Inclusions in Nephrite Jade from Xinjiang, Northwest China: Implications for Nephrite Jade Formation Temperatures. *Minerals* **2023**, *13*, 1403. [CrossRef]
28. Dai, L.-L.; Jiang, Y.; Yang, M.-X. Study on the Spectral Identification Characteristics of "Heiqing" and "Heibi". *Guangpuxue Yu Guangpu Fenxi Spectrosc. Spectr. Anal.* **2021**, *41*, 292–298. [CrossRef]
29. Han, D.; Liu, X.F.; Liu, Y. Formation and Coloration Factors of marble-type Hetian Jade in Hetian Region of Xinjiang. *Acta Petrol. Mineral.* **2018**, *37*, 1011–1026. (In Chinese with English Abstract)
30. Peng, F.; Zhao, Q.H.; Pei, L. Study of Mineralogy and spectral characteristics of Dahua black Nephrite from Dahua in Guangxi. *Spectrosc. Spectr. Anal.* **2017**, *37*, 2237–2241. (In Chinese with English Abstract)
31. Fang, T. Characteristics and Genesis of Hetian Jade Gobi Materials in Southern Xinjiang. *J. Gems Gemol.* **2018**, *20*, 27–38. (In Chinese with English Abstract) [CrossRef]